Heliyon 9 (2023) e21005

Contents lists available at ScienceDirect

Heliyon

journal homepage: www.cell.com/heliyon

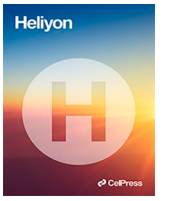

Electroacupuncture regulates hepatic cholesterol synthesis by HMGCR deubiquitination in rats

Shu-wen Jin [a], Yong-li Han [a], Xiao-li Pan [a,**], Hong-xing Zhang [a,b,*]

[a] College of Acupuncture and Orthopedics, Hubei University of Chinese Medicine, Wuhan, Hubei, 430061, China
[b] School of Medicine, Jianghan University, Wuhan, Hubei, 430056, China

ARTICLE INFO

Keywords:
Hyperlipidemia
Hepatic cholesterol synthesis
Electroacupuncture
Deubiquitination
Recombinant 3-hydroxy-3-Methylglutaryl coenzyme A reductase

ABSTRACT

This experiment was designed to explore the effect and mechanism of electroacupuncture (EA) for hyperlipidemia and hepatic cholesterol synthesis in rats. Liver and adipose tissues were assessed histologically, and body and liver weight, serum and liver lipid levels, expression of mTOR/ubiquitin-specific peptidase 20 (USP20)/recombinant 3-hydroxy-3-methylglutaryl coenzyme A reductase (HMGCR), and phosphorylation of mTOR and USP20 were measured. *In vitro* deubiquitination assays with liver cytosol were conducted. EA at Fenglong point ameliorated hyperlipidemia and hepatocyte steatosis, and decreased *p*-USP20, *p*-mTOR and HMGCR expression in the liver by reducing deubiquitination. Furthermore, EA decreased feeding-induced lipid biosynthesis in the liver. Concomitantly, EA prevented the induction of phosphorylated USP20 and mTOR, and HMGCR expression; and reduced the deubiquitination of HMGCR after refeeding. This experiment demonstrated that EA can effectively improve hyperlipidemia and reduce hepatic cholesterol synthesis by counteracting the deubiquitination activity of HMGCR in hyperlipidemic rats.

1. Introduction

Hyperlipidemia is characterized by abnormal blood lipid levels, specifically manifested as an increase in total cholesterol (TC), triglycerides (TG), or low-density lipoprotein cholesterol (LDL-C); and/or a decrease in high-density lipoprotein cholesterol (HDL-C) [1]. Excessive lipid levels in the bloodstream and the continuous accumulation of lipids in the liver, blood vessels, heart, and other organs leads to a variety of pathological changes such as inflammation, oxidative stress, and insulin resistance, which further induce a wide range of diseases such as non-alcoholic fatty liver disease (NAFLD), diabetes, metabolic disease, obesity, atherosclerosis, and cardiac dysfunction [2–6].

The human body requires approximately 1 g of TC per day [7]. Excessive lipid intake is an important factor in hyperlipidemia. Recent research has found that there is an mTOR/ubiquitin-specific peptidase 20 (USP20)/recombinant 3-hydroxy-3-methylglutaryl coenzyme A reductase (HMGCR) axis in the liver that can stabilize HMGCR by deubiquitination and promote cholesterol synthesis [8]. This axis was chronically activated in the liver of mice fed long-term with a high-fat high-sugar (HFHS) diet, further inducing hepatic

* Corresponding authorCollege of Acupuncture and Orthopedics, Hubei University of Chinese Medicine, No. 188 Tanhualin Road, Wuhan, Hubei 430061, China
** Corresponding authorCollege of Acupuncture and Orthopedics, Hubei University of Chinese Medicine, No. 188 Tanhualin Road, Wuhan, Hubei 430061, China
E-mail addresses: pxlzhenjiu@163.com (X.-l. Pan), zhxzhenjiu@163.com (H.-x. Zhang).

https://doi.org/10.1016/j.heliyon.2023.e21005
Received 20 May 2023; Received in revised form 25 September 2023; Accepted 12 October 2023
Available online 17 October 2023

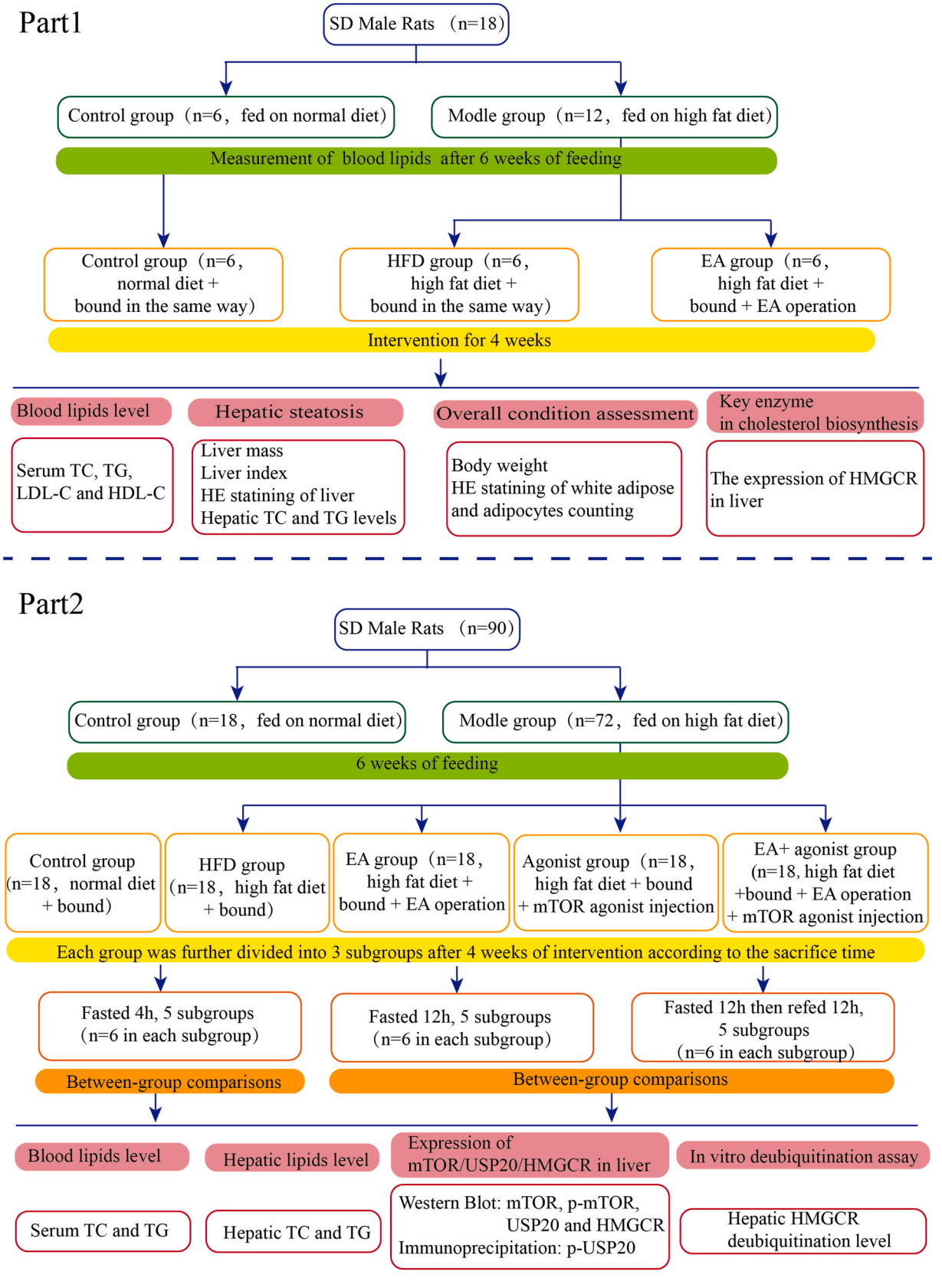

(caption on next page)

Fig. 1. Flow chart of the experimental design.

lipid synthesis. In addition, as this axis is a specific reflection of the transition between fasting and re-feeding, re-feeding induced a significantly higher mTOR signaling response and higher HMGCR levels in the HFHS-fed group compared with control mice. This in turn further worsened metabolic diseases, specifically manifested as obesity, accumulation of white adipose tissue and liver fat, and high lipid levels. Owing to its important role in liver metabolism, mTOR/USP20/HMGCR is an attractive molecular target for the treatment of hyperlipidemia.

Several clinical experiments have confirmed the effectiveness of electroacupuncture (EA) in the treatment of hyperlipidemia, with the ST40 (Fenglong point) being the most frequently used point in clinical practice [9,10]. A large number of animal studies have confirmed that EA has an effect on cholesterol metabolism, specifically on cholesterol reverse transport, LDL receptor levels, and cholesterol synthesis. Wu et al. showed that EA can downregulate HMGCR mRNA and protein expression in the liver, inhibit liver cholesterol synthesis, and reduce serum TC and LDL-C levels [11].

However, it is unclear whether EA can reduce HMGCR protein expression by downregulating deubiquitination and reduce hepatic lipid synthesis by mTOR/USP20/HMGCR axis in fasting/re-feeding paradigm.

Based on the results described above, we speculated that EA may reduce the chronic activation of the mTOR/USP20/HMGCR axis in hyperlipidemic rats and play a role in the downregulation of the mTOR/USP20 axis in the fasting/re-feeding paradigm by decreasing HMGCR deubiquitination and protein expression after re-feeding, thereby inhibiting liver cholesterol synthesis and lowering lipid levels in the bloodstream.

2. Materials and methods

2.1. Animals and diets

Specific-pathogen-free (SPF) male Sprague-Dawley rats (110–120 g) were purchased from Hubei Laboratory Animal Research Center and raised under SPF conditions, with a temperature of 20 ± 2 °C, a humidity of 50 ± 5 %, and a light/dark cycle of 12 h, with *ad libitum* access to food and water. The experiment was conducted in two parts. In the first part of the experiment, after three days of adaptive feeding, the rats were divided into a control and a model group, with six rats in the control group and twelve rats in the model group. The rats in the control group were fed a normal diet, whereas those in the model groups were fed a high-fat diet (HFD) (HFD: 77.5 % basic feed, 10 % lard oil, 10 % egg yolk powder, 2 % cholesterol, and 0.5 % sodium cholate; Wuhan Chunyuhong Laboratory Animal Feed Co., Ltd.) for six weeks. Ten percent of the energy was obtained from fat in the normal diet, whereas this percentage was 55 % in the HFD. After six weeks, blood samples were collected from the retro-orbital venous plexus, and serum lipids (TC, TG, LDL-C, HDL-C) were measured to evaluate whether the hyperlipidemia model had been well established. After six weeks of modeling, rats in model group were divided into a HFD group and a EA group, with six rats in each group. Those in the EA group were treated bilaterally with EA at the bilateral Fenglong point five times per week during four weeks. Rats in the control and HFD groups were instead handled and restrained for 30 min each day.

In the second part of the experiment, 90 rats were purchased and divided into a control and a model group. The control group was fed a normal diet, and the model group was fed a HFD for six weeks. The model group was then subdivided into a HFD group, an EA group, an agonist group, and an EA + agonist group, with 18 rats per group. Rats in the agonist and EA + agonist groups were treated with an mTOR agonist (L-leucine, HY-N0486, dissolved in saline; 18 g/l, 0.45 g/kg BW) via daily gavage. The same volume of saline was administered to the remaining rats. According to Ishiguro et al., the expression of phosphorylated mTOR (*p*-mTOR) in the rat liver increases significantly 1 h after intragastric administration of leucine [12]. Rats in the EA + agonist group and in the EA group received daily treatment with EA 1 h after the intragastric administration of leucine or saline, respectively. Those in the control, HFD, and agonist groups were handled and restrained instead, with the same schedule. After four weeks of treatment, six rats from each experimental group were sacrificed after 4 h of fasting, another six after 12 h of fasting, and the remaining six were sacrificed after re-feeding with a HFD for 12 h followed by fasting for 12 h. All experimental procedures followed the guidelines of the Hubei Animal Ethics Committee (hucms202204027). The flow chart detailing the experimental design is shown in Fig. 1.

2.2. EA treatment

During the EA treatment, the rats were conscious and restrained using a homemade restraining device. Stainless steel needles (0.18 mm × 10 mm, Yunlong Brand, Wujiang Yunlong Medical Equipment Co., Ltd., Wujiang, China.) were inserted bilaterally with a depth of approximately 7 mm at the Fenglong point, which is located at the middle fibula and that approximate 7 mm below the caput fibula [13]. Both Fenglong points were connected to a Han's Acupoint Nerve Stimulator (HANS-200A, Nanjing Jisheng Medical Technology Co., Ltd., Nanjing, China), which was used to provide electrical impulses with an alternating frequency of 2/100 Hz and an intensity of 1 mA, and produced slight twitching of the limbs [14]. The EA treatment lasted 30 min and was administered five times per week for 4 weeks.

2.3. Blood and liver biochemical assays

Blood samples were placed in a 1.5 mL EP tube for 2 h and centrifuged at 3000 rpm for 10 min. The supernatant was collected and

stored at −80 °C. Serum TC, TG, HDL-C, and LDL-C levels were determined using an automatic biochemical analyzer (Model BK280, BioBase, Inc., Jinan, Shandong, China). Liver samples (50 mg) were homogenized in 1 mL of isopropanol and centrifuged at 3500 rpm for 10 min. Then the supernatants (contained extracted TC and TG) were collected [15]. Hepatic TC and TG levels were measured using the total TC kit (Solarbio, BC1985) and TG kit (Solarbio, BC0625), respectively, according to the manufacturer's instructions.

2.4. Histopathological analyses

Liver and perirenal adipose tissues were collected and fixed in 4 % paraformaldehyde for more than 24 h, followed by dehydration with ethanol. The tissues were then embedded in paraffin and sliced into sections with a thickness of 3–5 μm. All sections were stained with Harris hematoxylin (H)/glacial acetic acid solution, de-stained with 1:400 v/v HCL/ethanol (70 %) solution, and stained with Eosin (E). The sections were then dehydrated with ethanol and xylene. A mounting media was added and the sections were covered with a coverslip. The arrangement of hepatocytes as well as hepatocyte steatosis and the presence of lipid droplets was observed using an optical microscope at 200 × magnification. The number of adipocytes per unit area was measured using Image-Pro plus 6.0 (Media Cybernetics, Inc., Rockville, MD, USA).

2.5. Western blotting

HMGCR, mTOR and *p*-mTOR expression levels were determined by Western blotting. Lysate buffer was added to the liver tissue collected from six rats in each group to extract total protein. Prepare 10 % separation gel and 5 % concentrated gel, fill the gel immediately after adding TEMED then start electrophoresis and transfer. After blocking with 5 % non-fat dry milk/TBST, the membranes were incubated overnight at 4 °C with the following primary antibodies: HMGCR (1:1000; sc-271595; santa), mTOR (1:3000; 66888-1-Ig; Proteintech), or *p*-mTOR (1:1000; 67778-1-Ig; Proteintech). After washing, the membranes were incubated with horseradish peroxidase-conjugated secondary antibodies at 37 °C for 1 h. The resulting bands were detected and analyzed using a chemiluminescence system (ChemiDoc™XRS+, Bio-rad). GAPDH served as internal control, and protein expression levels were normalized to it.

2.6. Immunoprecipitation

As there are no commercially available *p*-USP20 antibodies, we used immunoprecipitation to detect USP20 and its *p*-Ser protein levels. Lysate buffer were added to rat liver tissue samples for cell lysis. The tissue lysate was centrifuged and the supernatant was collected. After the protein concentration was determined by BCA, the protein expression level was determined using the USP20 antibody as input. After diluting the USP20 antibody (17491-1-AP; Proteintech), protein A + G agarose beads were added and the tubes were rotated at 4 °C for 1 h, and then centrifuged at 4 °C for 5 min. The tissue lysate was added to the protein A + G agarose beads coupled with the USP20 antibody, and the samples were incubated overnight. After centrifugation, the supernatant was removed and the pellet was washed thrice with phosphate buffer saline (PBS). The pellet was then resuspended in loading buffer, boiled for 5 min and centrifuged again. The supernatant was collected, and the degree of USP20 phosphorylation was analyzed by Western blotting using anti-*p*-Ser antibodies (612546; BD Biosciences).

2.7. In vitro deubiquitination assay with liver cytosol

As described by Song et al., *in vitro* deubiquitination assays were conducted using liver cytosol. First, CHO cells were incubated at 37 °C for 12 h in 5 % CO_2 with 10 ml DMEM/F12 medium supplemented with 5 % fetal bovine serum (FBS) [8]. After being washed once with PBS, the cells were incubated at 37 °C overnight in DMEM/F12 medium supplemented with 5 % lipoprotein Deficient Serum (LPDS), 1 μM lovastatin, and 10 μM mevalonate. To induce HMGCR ubiquitination, these sterol-depleted CHO cells were cultured with or without 1 μg ml^{-1} 25-hydroxycholesterol (25-HC) in the presence of 10 μM MG132 for 2 h. Membrane fractions were isolated from cell homogenates and immunoprecipitated with anti-HMGCR antibody-coupled agarose. The resulting pellets were then incubated with liver cytosol samples obtained from the experimental animals for 30 min at 37 °C, and the reaction was stopped by adding loading buffer, followed by SDS–PAGE and analysis by immunoblotting. In simple terms, the HMGCR deubiquitination level in the liver is reflected by the effect of liver tissue on the degree of HMGCR ubiquitination.

2.8. Statistical analysis

The sample size was determined based on previous studies in the field [8,16]. All data are presented as mean ± standard deviation. Statistical analyses were performed using GraphPad Prism v.9.3.1, or Microsoft Excel 2020. Data were analyzed by unpaired two-tailed Student's t-test, multiple unpaired *t*-test, or one-way analysis of variance (ANOVA) followed by Tukey's test, as described in the figure legends. Statistical significance was set at $P < 0.05$.

3. Result

3.1. Effects of EA on serum lipids

To investigate the effect of EA on hyperlipidemia *in vivo*, we established a rat model of long-term HFD-induced hyperlipidemia. After six weeks of HFD feeding, the serum TC, TG, and LDL-C levels in the HFD group were significantly increased compared with those in the control group (all $P < 0.01$), indicating that the hyperlipidemia model had been successfully established (Table 1).

As shown in Fig. 2A–D, after four weeks of EA treatment at Fenglong point, serum TC, TG and LDL-C in the EA group were significantly decreased compared with the HFD group, with TC decreasing by 21.02 % ($P < 0.01$), TG decreasing by 29.18 % ($P < 0.05$), and LDL-C decreasing by 14.98 % ($P < 0.05$). However, there were no significant differences in serum HDL among the three groups. The serum from rats in the control group was clear and transparent, with a light yellow color, whereas that from rats in the HFD group was turbid and milky white, due to the abundant presence of lipids. The serum from rats that received EA treatment was relatively clear and transparent (Fig. 2E). These results indicate that EA effectively ameliorated hyperlipidemia in rats fed with a HFD.

3.2. Effects of EA on hepatic lipid accumulation

As shown in Fig. 3A, the liver in rats from the control group appeared reddish-brown, with sharp edges and smaller in size, whereas the liver in those from the HFD group had yellowish surface with hypertrophic edges and intumescent tissue, indicating that chronic HFD induced hepatic steatosis and promoted fatty liver disease. The livers in rats that received EA treatment were light red. As clearly observed in slices with H&E staining (Fig. 3 B), the control group showed normal histological structures, in which the cells were arranged in an orderly manner and the hepatocytes were free of lipid droplets. HFD intake caused cell disarrangement and the presence of lipid droplets in hepatocytes, while EA treatment tended to make hepatocytes regularly arranged, with a lower number of lipid droplets and fatty degeneration, suggesting that EA almost completely reverses the process of hepatic steatosis. Although there was no significant difference in weight between the three groups ($P > 0.05$; Fig. 3C), the liver weight and liver index (liver index = liver mass/body weight) *100 %) in those groups showed a similar trend (Fig. 3D and E; $P < 0.01$ in both cases). The HFD group showed significantly increased liver weight and liver index compared with the control group ($P < 0.01$ in both cases). The rats that received EA treatment presented significantly lower values for these indicators ($P < 0.01$ in both cases). To quantitatively assess hepatic lipid accumulation, we measured TC and TG levels in the liver (Fig. 3F and G). The increased TC and TG in the liver induced by HFD intake were no longer evident in those animals that received EA treatment (37.4 % and 33.8 % of the corresponding values in the HFD group for TC and TG, respectively, $P < 0.01$ in both cases). These results demonstrate that EA directly reduced TC and TG levels in the liver, and efficiently reduced hepatic lipid accumulation in rats fed with a HFD.

Furthermore, we measured adipocyte size in the rats from each group. H&E staining of adipose tissue (Fig. 3H and I) shows that EA treatment significantly reduced the size of adipocytes and made their arrangement more compact compared with that of the HFD group. The adipocyte count showed the same trend in a quantitative way. The adipocyte area in the EA group decreased by approximately 40.08 % compared in the HFD group ($P < 0.01$), although it was still different from that of the control group.

3.3. Effects of EA on HMGCR deubiquitination by mTOR/USP20

To investigate the regulatory mechanism of EA in hepatic lipid biosynthesis, we measured the expression of the cholesterogenic rate-limiting enzyme HMGCR, which is also an important regulatory target. As shown in Fig. 4A and B, EA treatment substantially decreased HMGCR expression compared to that observed in the HFD group ($P < 0.01$). We performed an *in vitro* deubiquitylase (DUB) assay, as previously described by Songbaoliang [8]. HMGCR deubiquitination showed almost no change in the presence of liver cytosol in the control group, and was considerably increased by liver cytosol in the HFD group ($P < 0.01$), while EA treatment reversed this change ($P < 0.01$; Fig. 4C and D). To further identify the effect of EA on HMGCR deubiquitination, we measured protein levels of upstream components and their phosphorylation. As shown in Fig. 4E–G, the levels of HMGCR, phosphorylated USP20 (*p*-USP20), and *p*-mTOR were highly elevated in HFD-fed rats compared with those on a normal diet ($P < 0.01$), and EA treatment markedly alleviated these chronic activities on *p*-mTOR ($P < 0.05$) and *p*-USP20 ($P < 0.05$) and decreased HMGCR ($P < 0.01$). To verify the effect of EA on the downregulation of this signaling pathway, we treated rats with L-leucine by intragastric administration, and observed that the expression of *p*-mTOR, *p*-USP20, and HMGCR was increased compared with those in the HFD group (all $P < 0.05$). EA treatment also had a significant downregulation effect on the activation of this signaling pathway, as shown by the levels measured in the EA + agonist group (all $P < 0.05$).

Table 1
The blood lipids in control group and model group after 6 weeks of modeling.

Groups	TC (mmol/L)	TG (mmol/L)	LDL-C (mmol/L)	HDL-C (mmol/L)
Control	1.78 ± 0.19	0.98 ± 0.27	0.53 ± 0.09	1.31 ± 0.12
Model	2.57 ± 0.20**	1.76 ± 0.18**	0.81 ± 0.06**	1.22 ± 0.14

Data are expressed as the mean ± SD. $^{**}P < 0.01$, vs. control group.TC, total cholesterol; TG, triglycerides; LDL-C, low-density lipoprotein cholesterol; HDL-C, high-density lipoprotein cholesterol.

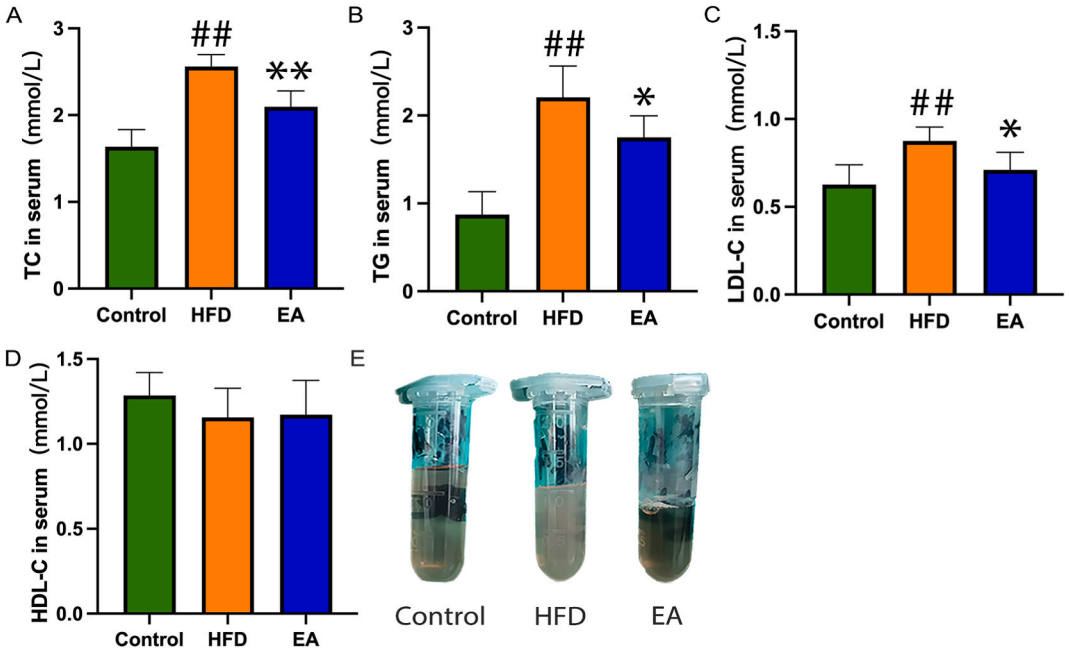

Fig. 2. Effects of EA on lipid levels in the serum. (A) TC levels. (B) TG levels. (C) LDL-C levels. (D) HDL-C levels. (E) A representative photograph of serum samples from the three experimental groups. Data are presented as mean ± SD. **P < 0.01, *P < 0.05, compared with HFD group. ##P < 0.01, compared with control group. TC, total cholesterol; TG, triglycerides; LDL-C, low-density lipoprotein cholesterol; HDL-C, high-density lipoprotein cholesterol; HFD, high fat diet; EA, electroacupuncture.

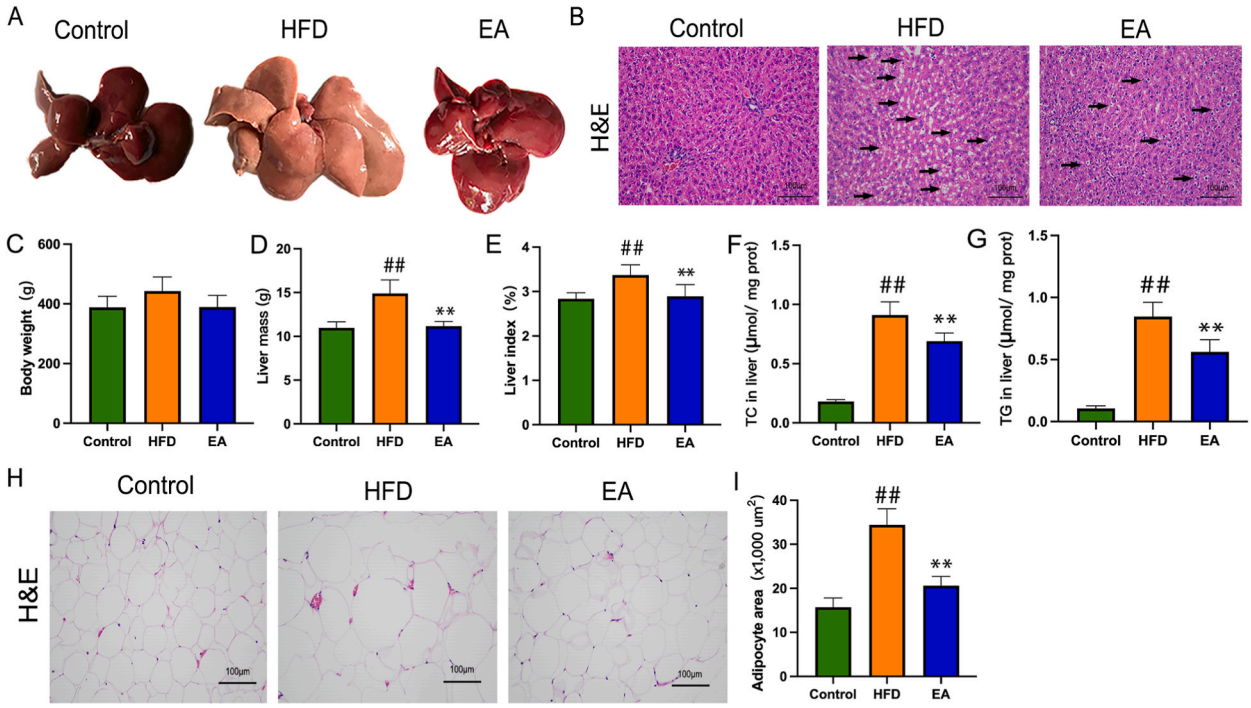

Fig. 3. Effects of EA on liver lipid accumulation and adipocyte size. (A) the whole liver. (B) Histological analysis of liver tissues by H&E staining (magnification: 200×). (C) body weight. (D) liver mass. (E) liver index. (F) TC in liver. (G) TG in liver. (H) histological analysis of adipocyte tissue by H&E staining. (I) Quantification of individual adipocyte size. All data are presented as mean ± SD. **P < 0.01, compared with HFD group. ##P < 0.01, compared with control group. TC, total cholesterol; TG, triglycerides; HFD, high fat diet; EA, electroacupuncture.

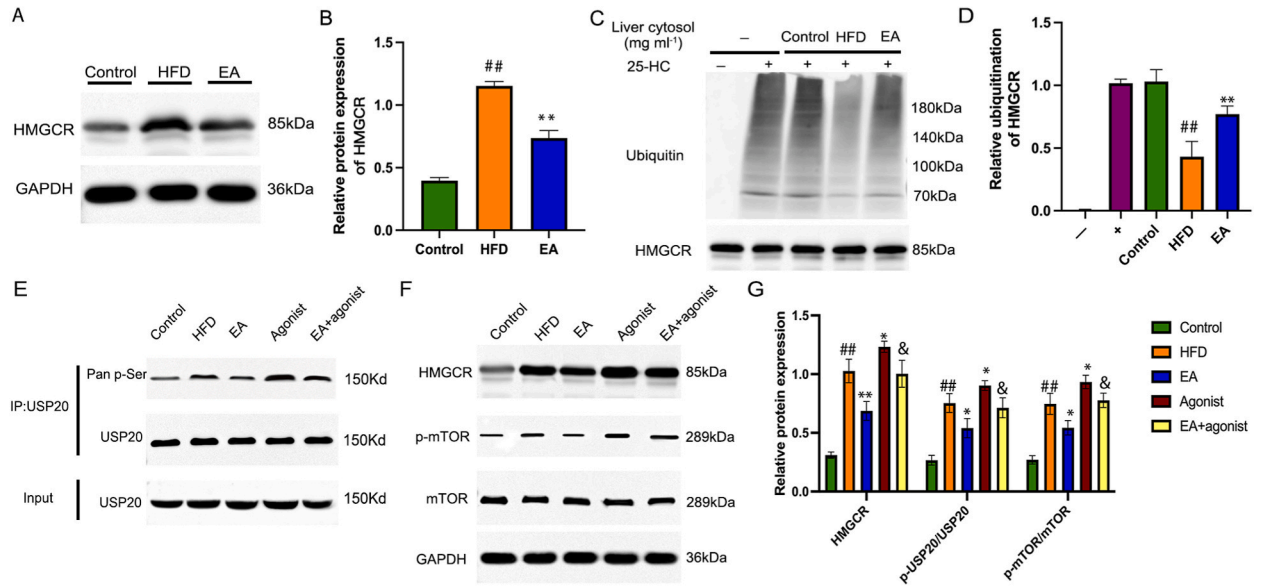

Fig. 4. Effect of EA on HMGCR deubiquitination. (A) Expression levels of HMGCR in the liver were detected by Western blot assay. GAPDH was used as a loading control. (B) Quantitative results for protein expression of HMGCR. (C) *In vitro* deubiquitination analysis of HMGCR. (D) Quantitative results for deubiquitination of HMGCR. (E) Western blot analysis of serine phosphorylation levels of USP20 pulled-down by immunoprecipitation. (F) Western blot analysis of mTOR, *p*-mTOR and HMGCR. (G) Quantitative results for protein expression of the components of the mTOR/USP20/HMGCR axis and their phosphorylation levels. All data are presented as mean ± SD. **P < 0.01, *P < 0.05, compared with HFD group. ##P < 0.01, compared with control group. &P < 0.05, compared with agonist group. HMGCR, recombinant 3-hydroxy-3-methylglutaryl coenzyme A reductase; USP20, ubiquitin-specific peptidase 20; HFD, high fat diet; EA, electroacupuncture.

3.4. Effects of EA on serum and liver lipids based on the mTOR/USP20/HMGCR axis

Next, we compared the serum and liver lipids among the five groups. Compared to the HFD group, serum TC and TG levels in the EA group were significantly reduced (P < 0.01in both cases). Rats in the agonist group exhibited higher serum TC (P < 0.05) and TG (P < 0.01) levels than those in the HFD group. The levels of serum TC (P < 0.05) and TG (P < 0.01) were remarkably reduced in the EA + agonist group but were still higher than those in the EA group (Fig. 5A and B). Similarly, EA significantly downregulated the levels of TC and TG in the liver of HFD rats (P < 0.01 in both cases), and the rats in the agonist group showed higher TC (P < 0.05) and TG (P < 0.01) levels in the liver than those in the HFD group. The EA + agonist group showed significantly decreased TC (P < 0.05) and TG (P < 0.01) levels in the liver, which were still higher than those in the EA group (Fig. 5C and D).

Considered together, all these data indicate that there was a chronic activity of *p*-mTOR and higher HMGCR deubiquitination activity by phosphorylating USP20 in hyperlipidemic rats on an HFD diet, increasing cholesterol biosynthesis in the liver, and inducing higher lipid levels in both liver and serum. EA can alleviate chronic activation of the mTOR/USP20/HMGCR axis, which protects HMGCR from ubiquitin-mediated proteasome degradation, thereby reducing the deubiquitination activity of HMGCR and reducing protein expression of HMGCR, further ameliorating hyperlipidemia and reducing hepatic lipid accumulation.

3.5. Effect of EA on the mTOR/USP20/HMGCR axis in a fasting/re-feeding paradigm

It has been demonstrated that feeding induces higher *p*-mTOR signaling to increase HMGCR deubiquitination via USP20 phosphorylation [8]. Owing to the chronic activity of *p*-mTOR, more USP20-mediated stabilization of HMGCR was observed in the HFD group than in the control group upon re-feeding. Based on this, we investigated the effect of EA on the mTOR/USP20/HMGCR axis in a fasting/re-feeding paradigm. As shown in Fig. 6A–E, the relative expression of HMGCR, *p*-USP20, and *p*-mTOR during re-feeding in all the groups was significantly increased compared to that measured in the fasted state (all P < 0.01). Furthermore, EA markedly decreased the relative expression of HMGCR (P < 0.01), *p*-USP20 (P < 0.05), and *p*-mTOR (P < 0.05) in the refed state compared to that in the HFD group. A similar trend was observed when the agonist and the EA + agonist groups were compared. In the EA + agonist group, the relative expression of HMGCR (P < 0.01), *p*-USP20 (P < 0.01), and *p*-mTOR (P < 0.05) was downregulated after re-feeding compared with the agonist group, in which the levels were higher than in the HFD group. Therefore, the induction of HMGCR, *p*-USP20, and *p*-mTOR by re-feeding was partially prevented by EA, with no effect on the levels of total USP20 and mTOR (P > 0.05).

Next, we performed an *in vitro* deubiquitination assay to identify the effect of EA on deubiquitination activity in the fasting/re-feeding paradigm. HMGCR deubiquitination was unchanged in the presence of liver cytosol from fasting rats in the five groups, and was substantially increased by the liver cytosol from re-fed rats in these groups to varying degrees (all P < 0.01). We observed lower HMGCR deubiquitination in the liver cytosol from rats in the EA group during re-feeding than in those from the HFD group (P <

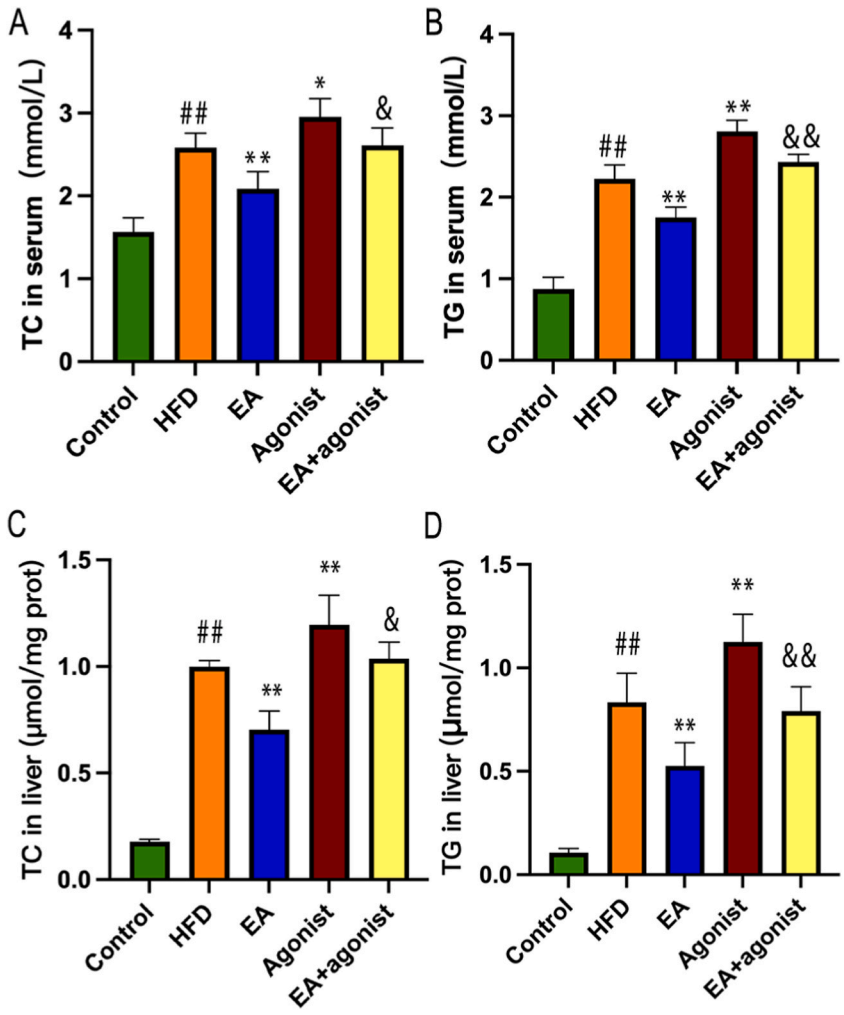

Fig. 5. Effects of EA on lipids in serum and liver. (A) TC in serum; (B) TG in serum. (C) TC in liver; (D) TG in liver. All data are presented as mean ± SD. **P < 0.01, *P < 0.05, compared with HFD group. ##P < 0.01, compared with control group. &&P < 0.01, &P < 0.05, compared with the agonist group. TC, total cholesterol; TG, triglycerides; HFD, high fat diet; EA, electroacupuncture.

0.01) (Fig. 6F and G). Compared with liver cytosol from re-fed HFD rats, liver cytosol from re-fed rats treated with the agonist caused more cleavage of HMGCR ubiquitin chains (P < 0.05). Concordantly, this change was reversed in the EA + agonist group (P < 0.01), causing increased HMGCR ubiquitination.

3.6. *Effect of EA on serum lipids and liver lipids in the fasting/re-feeding paradigm*

Re-feeding markedly increased serum TC and TG levels in all groups compared to those observed in fasting rats (all P < 0.01; Fig. 7A and B). Re-fed rats in the EA group showed lower serum TC and TG levels than in the HFD group (P < 0.01 in both cases). Re-fed rats in the agonist group exhibited higher serum TC (P < 0.05) and TG (P < 0.01) levels than those in the HFD group, and the higher serum lipid levels in the agonist group were reversed by EA treatment to some extent (P < 0.01 in both cases). Rats in all fasting groups showed similar results. During fasting, EA lowered liver TC and TG levels when compared to those from the HFD group, and the EA + agonist group showed a similar trend to that of the agonist group (Fig. 7C and D). Fasting liver TC was higher during fasting in the agonist group compared to the HFD group, but this was not the case for liver TG. Re-feeding decreased liver lipid levels in all groups (all P < 0.01). During re-feeding, liver TC (P < 0.01) and TG (P < 0.05) were remarkably lower in the EA group compared to the HFD group, and they were also lower in the EA + agonist group compared to the agonist group (P < 0.01). In contrast, liver TC (P < 0.01) and TG (P < 0.05) levels were both increased in the agonist group compared to the HFD group.

Together, these data indicated that EA ameliorated the increase in *p*-mTOR and *p*-USP20 in the HFD group during re-feeding and counteracted the deubiquitination activity of HMGCR induced by re-feeding (Figs. 6 and 7). EA decreased lipid biosynthesis in the liver induced by re-feeding, reduced the elevation of serum lipids after re-feeding, and further reduced lipid content in the liver (Fig. 8).

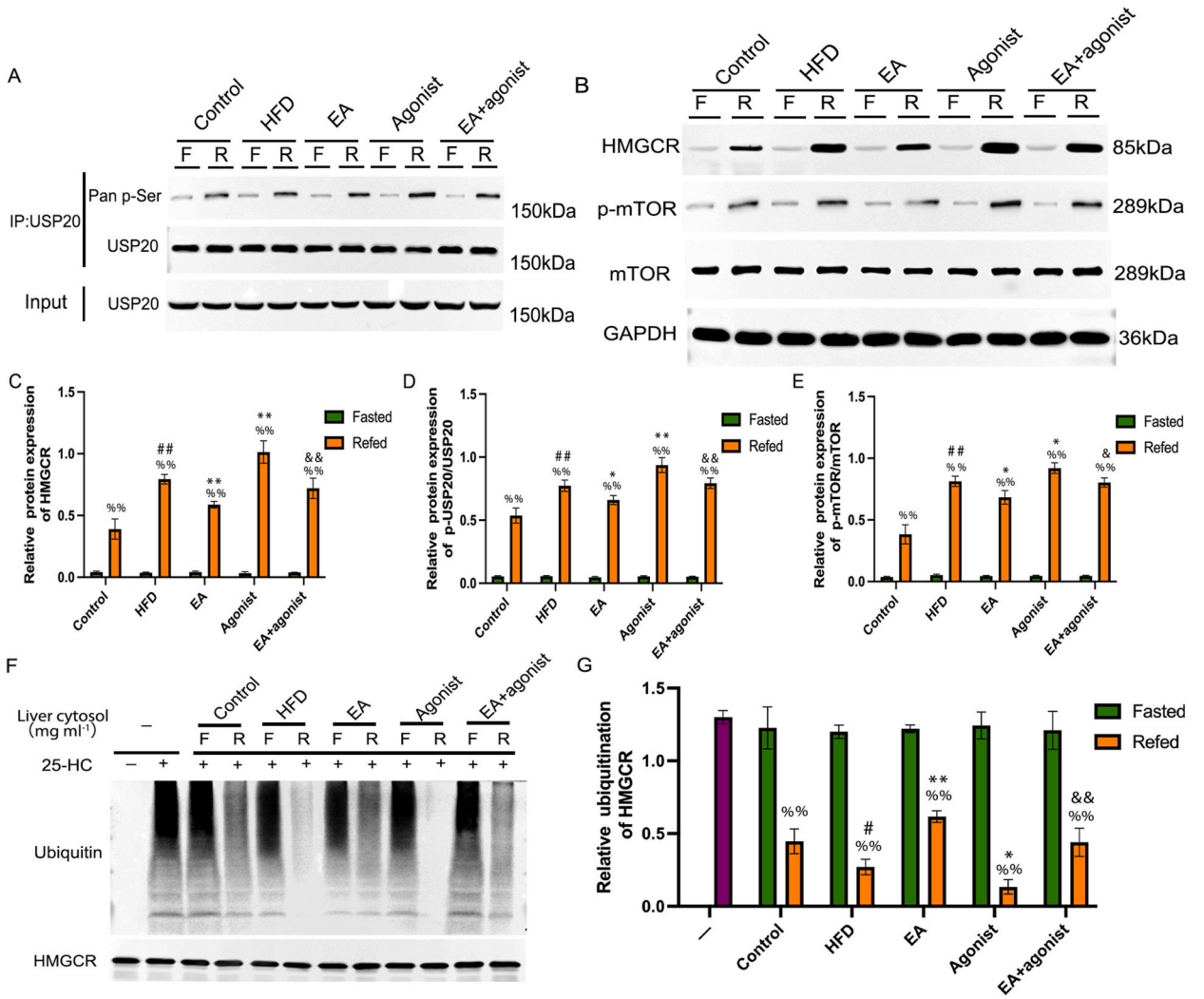

Fig. 6. Effect of EA on HMGCR deubiquitination in the fasting/re-feeding paradigm. (A) Western blot analysis of serine phosphorylation levels of immunoprecipitation USP20 pulled-down by immunoprecipitation (B) Western blot analysis of mTOR, *p*-mTOR and HMGCR levels (C–E) Quantitative results for the expression of HMGCR(C), *p*-usp20/usp20 (D) and *p*-mTOR/mTOR (E). (F) *In vitro* deubiquitination analysis of HMGCR (G) Quantitative results for deubiquitination of HMGCR. All data are presented as mean ± SD. **P < 0.01, *P < 0.05, compared with HFD group. ##P < 0.01, #P < 0.05, compared with control group. &&P < 0.01, &P < 0.05, compared with the agonist group. %%P < 0.01, compared with the fasting group. HMGCR, recombinant 3-hydroxy-3-methylglutaryl coenzyme A reductase; USP20, ubiquitin-specific peptidase 20; HFD, high fat diet; EA, electroacupuncture.

4. Discussion

Hyperlipidemia is an alteration of the plasma lipid profile, with hypercholesterolemia being the most common form [17]. High levels of TC and other lipids are closely associated with several diseases such as NAFLD, diabetes, obesity, and cardiovascular disease [18–20]. Mounting evidence demonstrates the beneficial effects of EA in lipid metabolism disorders such as hyperlipidemia, NAFLD, and cardiovascular disease [21–24]. We found that HFD intake during six weeks significantly increased TC, TG, and LDL-C levels in plasma (Table 1). EA can reduce TC, TG, and LDL-C levels, which its effectiveness in the regulation of lipids in plasma (Fig. 2).

The liver is the main site of cholesterol biosynthesis and delivers both endogenously synthesized and exogenously acquired cholesterol to the bloodstream [25]. Hyperlipidemia is strongly associated with NAFLD, and NAFLD may be driven by the predominant mechanisms for the development of hyperlipidemia [19,26]. Therefore, our study demonstrated the protective effects of EA against hepatic lipid accumulation. EA can inhibit lipid deposition in the liver, as demonstrated by gross observation of the liver and H&E staining. In addition, liver weight, liver index, and TC and TG levels in the liver were reduced after EA treatment. However, we did not observe any differences in body weight among the three groups. In addition, it has been shown that hypercholesterolemia induces adipocyte cholesterol overload, and further causes adipocyte hypertrophy, adipose tissue inflammation, and disruption of endocrine function, all of which might play a role in the development of chronic diseases such as obesity and metabolic syndrome [27–29]. Our

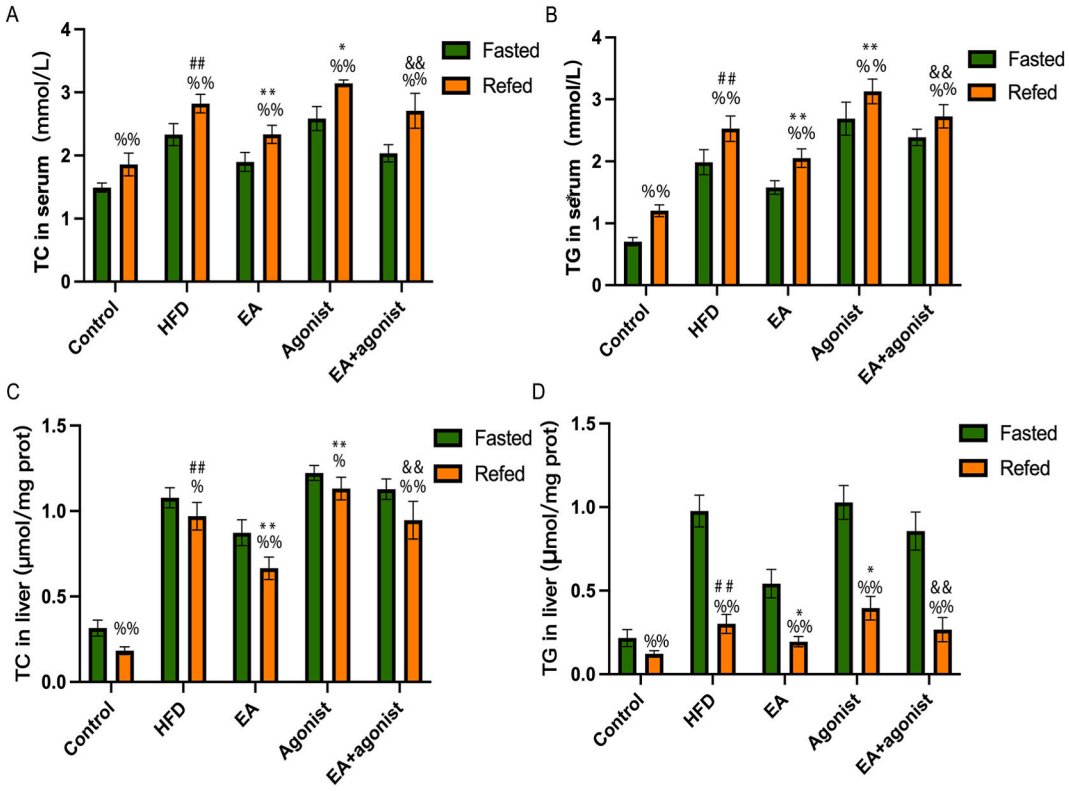

Fig. 7. Effects of EA on lipids in serum and liver in the fasting–refeeding paradigm. (A) TC in serum. (B) TG in serum. (C) TC in liver. (D) TG in liver. All data are presented as mean ± SD. **P < 0.01, *P < 0.05, compared with HFD group. ##P < 0.01, compared with control group. &&P < 0.01, compared with the agonist group. %%*P* < 0.01, %*P* < 0.05, compared with the fasting group. TC, total cholesterol; TG, triglycerides; HFD, high fat diet; EA, electroacupuncture.

study found that EA can significantly decrease the adipocyte area in rats fed with an HFD, and ameliorate adipocyte hypertrophy.

De novo biosynthesis is the major source of cholesterol in humans, with approximately 50 % of the total cholesterol synthesized in the liver [24]. HMGCR, the rate-limiting enzyme in cholesterol biosynthesis, is highly regulated at the transcriptional, translational, and post-translational levels to prevent toxicity caused by excess cholesterol [30]. In this study, we focused on the regulation of HMGCR stability and activity through post-translational modifications. When a sufficient amount of sterol accumulates in the cell, HMGCR is ubiquitinated and degraded by INSIG1 binding to the membrane domain of HMGCR and recruiting ubiquitin ligase gp78 [31]. A recent study explored deubiquitylase activity in livers from HFHS-fed mice through the mTOR/USP20/HMGCR axis, which protects HMGCR from ubiquitin-mediated proteasomal degradation and stabilizes cholesterol biosynthesis in the liver, exacerbating metabolic diseases such as hyperlipidemia, steatosis, obesity, and diabetes [8]. USP20 is the liver HMGCR deubiquitylase, which is phosphorylated by mTOR at S132 and S134 and then binds gp78, which stabilizes HMGCR by deubiquitination. There was much higher *p*-mTOR signaling and higher HMGCR levels by phosphorylating USP20 in HFHS-fed mice than in chow-fed mice [8]. A previous study reported that EA lowered serum lipids and HMGCR protein expression in the liver of hyperlipidemic rats [11]. However, our understanding of the mechanisms through which EA regulates HMGCR protein expression is limited. Therefore, we further explored the mechanism by which EA reduces lipid levels in serum and hepatic lipid synthesis by counteracting the chronic activation of HMGCR deubiquitination in rats fed with a HFD. We also focused on the deubiquitination activity of HMGCR and the phosphorylation of mTOR and USP20. According to a previous study, the mTOR/USP20/HMGCR axis in the liver can be generally reflected when rats were fasted for 4 h because the protein expression of HMGCR is closely related to the fasting and refeeding paradigm [8]. In this study, we observed decreased HMGCR levels, which is consistent with a previous study, and decreased deubiquitination of HMGCR in livers from the EA group, indicating that EA may reduce the protein expression of HMGCR by downregulating its deubiquitination activity. Furthermore, we demonstrated that EA downregulates the mTOR/USP20/HMGCR axis, and that this can be reversed by an mTOR agonist.

Additionally, compared with those from mice at the fasting stage, the mTOR/USP20/HMGCR signaling pathway is activated in livers from re-fed mice, and DUB activity is higher, which increases hepatic cholesterol synthesis in what is known as the fasting/re-feeding transition [8]. Long-term HFHS-fed mice remained more responsive to the fasting/re-feeding paradigm, displaying much higher levels of mTOR signaling and HMGCR levels by phosphorylating USP20 in the liver. To further verify the effect of EA on hepatic lipid synthesis in HFD-fed rats upon re-feeding, we compared the protein expression levels of the components of the mTOR/-USP20/HMGCR axis, the deubiquitination of HMGCR, and the lipid levels in serum and liver during the fasting and re-feeding phases

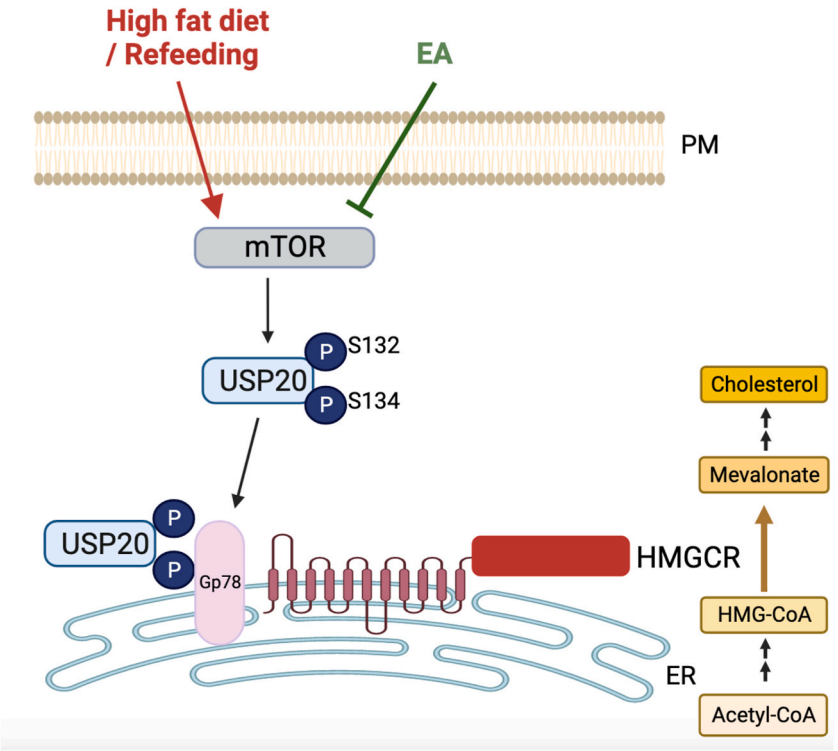

Fig. 8. Hypothesized mechanism of EA downregulation of mTOR/USP20 phosphorylation and counteraction of HMGCR deubiquitination activity in hyperlipidemia.

for each experimental group. According to Song's study, the longer the re-feeding time, the higher the protein expression of HMGCR, and the protein expression of HMGCR was increased by approximately 20-fold upon re-feeding for 12 h. Therefore, in this part of the experiment, the rats were fasted for 12 h and then sacrificed, and the re-fed rats were fasted for 12 h and then re-fed for 12 h and then sacrificed. In this study, we found that EA lowered the expression levels of the components of the mTOR/USP20/HMGCR axis and reduced the deubiquitination of HMGCR after re-feeding, both of which could be reversed by administration of an mTOR agonist. In parallel, EA reduced the elevated levels of serum TC and TG and decrease the hepatic TC and TG content in the fasting/re-feeding paradigm.

Statins, which can inhibit HMGCR enzymatic activity, are effective in lowering serum lipids and reducing the risk of cardiovascular disease. However, they also increase the risk of liver dysfunction, renal insufficiency, self-reported muscle symptoms, and eye conditions [32]. In addition, statins prevent adipocyte browning in mice, impair adipocyte protein prenylation, and induce new-onset diabetes in humans [33,34]. Acupuncture, an external therapy practiced for thousands of years in China and increasingly adopted worldwide, has been widely applied in treating hyperlipidemia and its related diseases. Clinical evidence suggests that acupuncture has a lipid-lowering effect that is similar to that of statins, with fewer adverse effects [35]. In addition to its lipid-lowering effect, EA also increases cholesterol efflux, reduces the release of inflammatory factors, and improves hemodynamics to prevent hyperlipidemia [16,36,37]. In terms of lipid-lowering effect, acupuncture not only inhibits the expression of HMGCR, but also suppresses the expression of hepatic sterol regulatory-element binding proteins [36]. Our study focused on the post-translational modifications of HMGCR and its mediation of hepatic lipid synthesis in a fasting/re-feeding paradigm.

4.1. Limitations

This study has some limitations. Firstly, alternative detection methods could have been used to determine the effect of EA on the rate of cholesterol synthesis, for instance, by calculating the amount of [^{3}H]-water incorporated into sterols per hour per gram of liver tissue. Secondly, the upstream mechanism of mTOR/USP20 by EA remains unclear. In the future, a more in-depth study should be conducted to further clarify the pathways by which EA regulates liver cholesterol metabolism.

5. Conclusion

The molecular mechanisms that underlie the hypolipidemic action of EA in hyperlipidemic rats may be mediated by downregulation of mTOR/USP20 phosphorylation and counteraction of HMGCR deubiquitination activity. In addition, we demonstrated the downregulation effect of EA on the mTOR/USP20/HMGCR axis in a fasting/re-feeding paradigm. This suggests an inhibitory effect of

EA on hepatic lipid synthesis in hyperlipidemic rats, and provides additional experimental evidence on EA as a potential treatment against hyperlipidemia.

Ethics statement

The present study was reviewed and approved by the Ethics Committee of the Hubei University of Chinese Medicine (approval code: hucms202204027).

Funding statement

This study was supported by the National Natural Science Foundation of China (Grant NO. 82274663), and the Science and Technology Research Program of the Hubei Provincial Department of Education (NO. Q20212008).

Data availability statement

Data will be made available on request.

CRediT authorship contribution statement

Shu-wen Jin: Data curation, Project administration, Writing – original draft, Writing – review & editing. **Yong-li Han:** Project administration. **Xiao-li Pan:** Funding acquisition, Supervision, Validation. **Hong-xing Zhang:** Data curation, Funding acquisition, Supervision, Validation.

Declaration of competing interest

The authors declare that they have no known competing financial interests or personal relationships that could have appeared to influence the work reported in this paper.

Appendix A. Supplementary data

Supplementary data to this article can be found online at https://doi.org/10.1016/j.heliyon.2023.e21005.

References

[1] S. He, Z. Xiong, L. Li, Y. Wang, C. Wang, B. Zheng, et al., Lotus seed resistant starch ameliorates high-fat diet induced hyperlipidemia by fatty acid degradation and glycerolipid metabolism pathways in mouse liver, Int. J. Biol. Macromol. 215 (2022) 79–91.
[2] J.H. Sun, Z.D. Wang, L. Chen, G.J. Sun, Hypolipidemic effects and preliminary mechanism of Chrysanthemum flavonoids, its main components luteolin and luteoloside in hyperlipidemia rats, Antioxidants 10 (2021) 1309.
[3] X. Si, J. Tian, C. Shu, Y. Wang, E. Gong, Y. Zhang, et al., Serum ceramide reduction by blueberry anthocyanin-rich extract alleviates insulin resistance in hyperlipidemia mice, J. Agric. Food Chem. 68 (2020) 8185–8194.
[4] L.G. Chen, X.W. Chen, X. Huang, B.L. Song, Y. Wang, Y.G. Wang, Regulation of glucose and lipid metabolism in health and disease, Sci. China Life Sci. 62 (2019) 1765–1775.
[5] D. Fan, L. Li, Z. Li, Y. Zhang, X. Ma, L. Wu, G. Qin, Effect of hyperlipidemia on the incidence of cardio-cerebrovascular events in patients with type 2 diabetes, Lipids, Health. Dis. 17 (2018) 102.
[6] Y.S. Yao, T.D. Li, Z.H. Zeng, Mechanisms underlying direct actions of hyperlipidemia on myocardium: an updated review, Lipids, Health. Dis. 19 (2020) 23.
[7] J.J. Repa, D.J. Mangelsdorf, The role of orphan nuclear receptors in the regulation of cholesterol biosynthesis, Annu. Rev. Cell Dev. Biol. 16 (2000) 459–481.
[8] X.Y. Lu, X.J. Shi, A. Hu, J.Q. Wang, Y. Ding, W. Jiang, et al., Feeding induces cholesterol biosynthesis via the mTORC1–USP20–HMGCR axis, Nature. 588(2030) 479-484.
[9] T.F. Zhang, W.J. Wan, H.X. Zhang, J.W. Li, G.W. Cai, L. Zhou, Multi-center observation of electroacupuncture at fenglong point in the treatment of hyperlipedemia, Chin, J. Clin. Reh. 10 (2006) 17–19.
[10] M. Liu, W. Hu, S. Xie, J. Zhang, Z. Zhao, X. Chang, Characteristics and laws of acupoints seclction in the treatment of hyperlipedemia with acupuncture and moxibustion, Chin. Acupunct. Moxibustion 35 (2015) 512–516.
[11] H. Wu, Based on Cholesterol Metabolism and Inflammation Mediated by SCAP/SREBP-2 Signaling Pathway to Explore the Effect of Electroacupuncture on Hyperlipidemia Rats, Hubei University of Chinese Medcine, Wuhan, China, 2021.
[12] H. Ishiguro, Y. Katano, I. Nakano, M. Ishigami, K. Hayashi, T. Honda, et al., Clofibrate treatment promotes branched-chain amino acid catabolism and decreases the phosphorylation state of mTOR, eIF4E-BP1, and S6K1 in rat liver, Life Sci. 79 (2006) 737–743.
[13] N.Y. Xue, D.Y. Ge, R.J. Dong, H.H. Kim, X.J. Ren, Y. Tu, Effect of electroacupuncture on glial fibrillary acidic protein and nerve growth factor in the hippocampus of rats with hyperlipidemia and middle cerebral artery thrombus, Neural, Regen. Res. 16 (2021) 137–142.
[14] M. Liu, Q. Zhang, Y. Guo, Efficacy and safety of acupuncture therapy in treating hyperlipidemia：A systematic review and meta-analysis of randomized controlled trials, Chin. General. Practice. 24 (2021) 4268–4275.
[15] M.S. Ferreira, S.C.P. D Luquetti, P.G.A. Brasiel, et al., Maternal soy protein isolate diet during lactation programs deleterious effects on hepatic lipid metabolism, atherogenic indices, and function of adrenal in adult rat offspring, J. Dev. Orig. Health. Dis. 13 (2022) 177–186.
[16] M. Yeom, J. Park, B. Lee, H.S. Lee, H.J. Park, R. Won, et al., Electroacupuncture ameliorates poloxamer 407-induced hyperlipidemia through suppressing hepatic SREBP-2 expression in rats, Life Sci. 203 (2018) 20–26.
[17] A. Pirillo, M. Casula, E. Olmastroni, G.D. Norata, A.L. Catapano, Global epidemiology of dyslipidaemias, Nat. Rev. Cardiol. 18 (2021) 689–700.
[18] L. Kopin, C.J. Lowenstein, Dyslipidemia, Ann. Intern. Med. 167 (2017) ITC81–ITC96.

[19] V.T. Samuel, K.F. Petersen, G.I. Shulman, Lipid-induced insulin resistance: unravelling the mechanism, Lancet 375 (2010) 2267–2277.
[20] E.E. Powell, V.W. Wong, M. Rinella, Non-alcoholic fatty liver disease, Lancet 397 (2021) 2212–2224.
[21] Z.X. Li, Y.L. Xie, W. Yi, H.H. Zhang, X.R. Tang, X.X. Liu, et al., Clinical therapeutic effect of hyperlipidemia of turbid phlegm obstruction pattern/syndrome treated with the different Jin's three-needle therapies, Zhen. Ci, Yan. Jiu. 44 (2019) 916–921.
[22] Y. Bi, B. Yin, G. Fan, Y. Xia, J. Huang, A. Li, et al., Effects of acupoint therapy on nonalcoholic fatty liver disease: a systematic review and meta-analysis, Complement, Ther. Clin. 43 (2021), 101376.
[23] X. Ke, Q. Xiang, P. Jiang, W. Liu, M. Yang, Y. Yang, et al., Effect of electroacupuncture on short-chain fatty acids in peripheral blood after middle cerebral artery occlusion/reperfusion in rats based on gas chromatography-mass spectrometry, Mediat. Inflamm. (2022) 3997947.
[24] N.Y. Xue, D.Y. Ge, R.J. Dong, H.H. Kim, X.J. Ren, Y. Tu, Effect of electroacupuncture on glial fibrillary acidic protein and nerve growth factor in the hippocampus of rats with hyperlipidemia and middle cerebral artery thrombus, Neural, Regen. Res. 16 (2021) 137–142.
[25] J. Luo, H. Yang, B.L. Song, Mechanisms and regulation of cholesterol homeostasis, Nat. Rev. Mol. Cell. Bio 22 (2020) 225–245.
[26] A. Pirillo, M. Casula, E. Olmastroni, G.D. Norata, A.L. Catapano, Global epidemiology of dyslipidaemias, Nat. Rev. Cardiol. 18 (2021) 689–700.
[27] J. Sun, Z. Wang, L. Chen, G. Sun, Hypolipidemic effects and preliminary mechanism of Chrysanthemum flavonoids, its main components luteolin and luteoloside in hyperlipidemia rats, Antioxidants 10 (2021) 1309.
[28] D. Aguilar, M.L. Fernandez, Hypercholesterolemia induces adipose dysfunction in conditions of obesity and nonobesity, Adv. Nutr. Res. 5 (2014) 497–502.
[29] C.R. Kahn, G. Wang, K.Y. Lee, Altered adipose tissue and adipocyte function in the pathogenesis of metabolic syndrome, J. Clin. Invest. 129 (2019) 3990–4000.
[30] J.L. Goldstein, M.S. Brown, Regulation of the mevalonate pathway, Nature 343 (1990) 425–430.
[31] B.L. Song, N. Sever, R.A. DeBose-Boyd, Gp78, a membrane-anchored ubiquitin ligase, associates with Insig-1 and couples sterol-regulated ubiquitination to degradation of HMG CoA reductase, Mol. Cell. 19 (2005) 829–840.
[32] T. Cai, L. Abel, O. Langford, G. Monaghan, J.K. Aronson, R.J. Stevens, et al., Associations between statins and adverse events in primary prevention of cardiovascular disease: systematic review with pairwise, network, and dose-response meta-analyses, BMJ (2021) 374.
[33] M. Paseban, A.E. Butler, A. Sahebkar, Mechanisms of statin-induced new-onset diabetes, J. Cell. Physiol. 234 (2019) 12551–12561.
[34] M. Balaz, A.S. Becker, L. Balazova, L. Straub, J. Müller, G. Gashi, et al., Inhibition of mevalonate pathway prevents adipocyte browning in mice and men by affecting protein prenylation, Cell. Metab. 29 (2019) 901–916.
[35] H.X. Zhang, H. Wu, H. Huang, Y. Xiao, D. Wang, Effects of electroacupuncture stimulation of "Fenglong" (ST 40) on expression of liver ATP-binding cassette transporterA1 mRNA and protein in rats with hyperlipidemia, Zhen. Ci. Yan. Jiu. 38 (2013) 100–105.
[36] Z.K. Yan, Z.J. Yang, F. Chen, Effect of electroacupuncture intervention on blood-lipid, high-sensitivity C-reactive protein and adiponectin levels in hyperlipidemia rats, Zhen. Ci. Yan. Jiu. 38 (2013) 365–368.
[37] W. Le, Y. Xiao, J.Y. Tian, Y.F. Chen, H. Jin, W. Ma, Effect of electroacupuncture at fenglong (ST40) on expressions of inflammatory factors in macrophages of hyperlipidemia model rats, Zhong. Guo. Zhong. Xi. Yi. Jie. He. Za. Zhi. 33 (2013) 1361, 1316.